A Comparison of Standard and Hybrid Classifier Methods for Mapping Hardwood Mortality in Areas Affected by "Sudden Oak Death"

Maggi Kelly, David Shaari, Qinghua Guo, and Desheng Liu

Abstract

The sudden oak death (SOD) epidemic in California has resulted in hundreds of thousands of dead trees in the complex of oak (Quercus) *and tanoak* (Lithocarpus) *woodland that exist in patches along the California coast. Monitoring SOD occurrence and spread is an on-going necessity in the state. Remote sensing methods have proved to be successful in mapping and monitoring forest health and distribution when a sufficiently small ground resolution is used. Supervised, unsupervised, and "hybrid" classification methods were evaluated for their accuracy in discriminating dead and dying tree crowns from bare areas and the surrounding forest mosaic utilizing 1-m ADAR imagery covering both tanoak/redwood forest and mixed hardwood stands. In both study areas the hybrid classifier significantly outperformed the other methods, producing low omission and commission errors among information classes. The hybrid method was then further refined by varying three parameters of the algorithm (iteration number, homogeneity threshold, and number of classes) and accuracy was assessed. The results demonstrate that while the hybrid method outperformed the other classifiers, the parameters that yielded highest accuracy for the algorithm differed between the two study areas. The use of a randomly selected subsample of training pixels was compared to the use of polygonal training areas, and we found that polygonal training data provided better classification accuracies in both cases.*

Introduction

Sudden Oak Death

The newly discovered pathogen, *Phytophthora ramorum*, has been killing hundreds of thousands of tanoak (*Lithocarpus densiflorus*), coast live oak (*Quercus agrifolia*), and black oak (*Quercus kelloggii*) trees in California since it was first reported in 1995 (Rizzo, *et al.*, 2002). The seemingly rapid decline of the symptomatic trees has led to the disease complex name "sudden oak death" (SOD) (Rizzo and Garbelotto, 2003). As of May 2003, the disease has officially been confirmed in 12 coastal counties of California, reaching epidemic proportions in areas along approximately 300 km of the central California coast (Figure 1) (Rizzo and Garbelotto, 2003). Hosts for the disease exist across the state and SOD has also been detected on 40 acres in Southern Oregon. Marin County, California is one of the "hot-spots" for SOD, with several areas including the Marin Municipal Water District (MMWD) and China Camp State Park (CCSP) displaying extensive mortality of tanoaks, coast live oaks, and black oaks (Rizzo and Garbelotto, 2003). Monitoring the disease through time is critical for management of the disease and for further elucidating disease spread patterns (Kelly and McPherson, 2001).

There are numerous examples of the utility of remotely sensed data analysis to monitor forest health. Most of this work has examined conifer forests, although remote sensing of hardwood forests is also performed to look at structure and health (Boyer, *et al.*, 1988; Everitt, *et al.*, 1999; Gong, *et al.*, 1999; Muchoney and Haack, 1994). The pathology of this new disease affords an opportunity for continued development of techniques for remote sensing in hardwood forests, and indeed, remote sensing is a component of the statewide SOD monitoring plan for California (Kelly and McPherson, 2001). Specifically, the disease has several characteristics that make a monitoring approach that combines remote sensing and fieldwork ideal (Kelly, 2002). The affected *Quercus* species, and the larger, overstory *Lithocarpus* individuals make good targets for high-resolution imagery. Average crown diameter for affected *Quercus* species here is approximately 3 m and for the *Lithocarpus* species it is approximately 2 m. In addition, as diseased trees die, the entire crown changes dramatically from healthy green to brown over a short time period (in most cases) (Rizzo and Garbelotto, 2003). Moreover, in areas where SOD is advanced, the affected trees are clustered in groups 200–500 m in diameter (Kelly and Meentemeyer, 2002), resulting in dramatic spectral reflectance changes across larger areas, facilitating identification of the disease using remote sensing techniques. These characteristics are shown in Plate 1. Despite these obvious and dramatic visual characteristics associated

Maggi Kelly, Qinghua Guo, and Desheng Liu are with the Department of Environmental Sciences, Policy and Management, University of California, Berkeley and the Center for the Assessment and Monitoring of Forest and Environmental Resources (CAMFER). 145 Hilgard Hall, #3114. Berkeley, CA 94720-3114 (mkelly@nature.berkeley.edu).

David Shaari is with the Center for the Assessment and Monitoring of Forest and Environmental Resources (CAMFER). University of California, Berkeley, 145 Hilgard Hall, #3114. Berkeley, CA 94720-3114 (dshaari@nature.berkeley.edu).

Photogrammetric Engineering & Remote Sensing
Vol. 70, No. 11, November 2004, pp. 1229–1239.

0099-1112/04/7011–1229/$3.00/0
© 2004 American Society for Photogrammetry and Remote Sensing

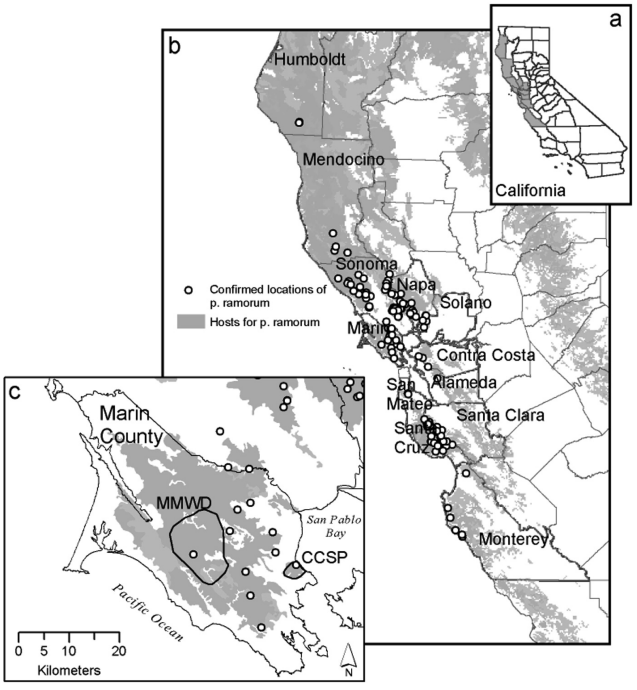

Figure 1. Sudden oak death in California: (a) the counties with confirmed SOD, and locations of positive samples; (b) state-wide with the distribution of susceptible host species; and (c) Marin County, showing the study area and the possible range of host species within the county.

with the disease, automated classification of tree mortality from remotely sensed imagery is not a straightforward process and is complicated by many factors, including confusion with bare areas. Seasonality, species morphology differences and spatial resolution should be considered when mapping hardwood mortality. Indeed, successful mapping of dead crowns in Marin County, California using high spatial resolution imagery has only been possible to date using post-classification map refinement through spatial querying and editing (Kelly and Meentemeyer, 2002; Kelly, 2002).

Spectral Classification Methods

Image classification is the process of grouping image data into classes with similar spectral values, which are assigned to meaningful information classes (Wayman, *et al.*, 2001). Development of algorithms for image classification has continued for several decades (Jensen, 1996). The classification process commonly involves the creation of spectral signatures for information classes which are used to classify the image pixel by pixel. Classification methods for remotely sensed imagery are commonly categorized into supervised and unsupervised forms (Lillesand and Kiefer, 2000). Supervised classification involves choosing representative training pixels from a pre-defined classification scheme that then are used with a decision rule (e.g., minimum distance, maximum likelihood, and Mahalanobis distance) to assign spectral data to information classes (Erdas, 1999; Jensen, 1996; Lillesand and Kiefer, 2000). Supervised classification methods partition the image space into classes that are separable and, in the case of maximum likelihood classifier, normally distributed. Supervised classification methods have been labeled as overly subjective (Martinez-Casasnovas, 2000) and difficult to correctly implement, as user-defined classes may not be normally distributed (Jensen, 1996), or there may be classes that are unknown to the analyst before classification (Martinez-Casasnovas, 2000).

Differences in training data collection in supervised classification (e.g., by pixel, seeded polygon, or block polygon) can produce differences in classification results, especially at high spatial resolutions (Chen and Stow, 2002). This is commonly explained by the fact that pixels from polygonal training data are autocorrelated, and thus can be under-representative of an information class (Campbell, 1981; Muchoney and Strahler, 2002). It has been suggested that non-contiguous single pixel training data avoids autocorrelation effects, provides higher variance, and thus produces more accurate classifications (Campbell, 1981; Gong and Howarth, 1990). This suggestion has recently been investigated with high resolution imagery (Chen and Stow, 2002), and these concerns make supervised classifiers and others that require *a priori* training data somewhat problematic. Despite these drawbacks, supervised classification and its variants continue to be used across a wide range of spatial resolutions and applications including vegetation mapping using AVHRR (Muchoney and Strahler, 2002), fire mapping using Landsat ETM imagery (Miller and Yool, 2002), and urban land use mapping using high resolution digital imagery (Barr and Barnsley, 2000).

Conversely, unsupervised classification methods require minimum initial training data; the classification algorithm searches for natural groupings in the data. After clustering, the analyst has to *a posteriori* label the found spectral classes as desired information classes. ISODATA (Iterative Self-Organizing Data Analysis Technique) is a standard unsupervised classifier (Jensen, 1996) that uses minimum spectral distance to assign a cluster for each candidate pixel through a number of iterations (Erdas, 1999). The user specifies a convergence threshold, number of desired classes, and number of iterations. Iterations cease when either the convergence threshold or the maximum number of iterations is reached. While avoiding the subjectivity and autocorrelation effects inherent in pre-classification training selection (Campbell, 1981; Jensen, 1996), the ISODATA method is not completely automated, as it requires that the analyst manually label the resultant spectral classes to information classes. Unsupervised methods, especially ISODATA, continue to be a popular choice for analysts without extensive *a priori* field knowledge (e.g., for classifying historical or time-series data (Lucas, *et al.*, 2000; Wang, *et al.*, 2002)), or for those wanting to avoid introduced bias in classification analysis. As with the supervised methods described above, unsupervised applications range broadly in context and scale; unsupervised methods have been successful in mapping vegetation using AVHRR, TM or ETM imagery in several studies (Egbert, *et al.*, 2002; Lucas, *et al.*, 2000; Lunetta, *et al.*, 2002; Xiao, *et al.*, 2002).

Comparisons between supervised and unsupervised methods have been inconclusive across spatial resolutions. Several studies report the benefits of supervised methods over unsupervised alternatives (Frazer, 1998; Miller and Yool, 2002; Nagendra and Gadgil, 1999), while others report the reverse, or results that are inconclusive (Bryant and Huber, 1998; Lass and Callihan, 1997; Thomson, *et al.*, 1998). Miller and Yool (2002) found that while an unsupervised method on multitemporal TM data was better at fire scar delimitation on a change image than manual airphoto interpretation, a supervised approach outperformed it. Nagendra and Gadgil (1999) reported that maximum likelihood classification of the Indian Remote Sensing Satellite (IRSS) imagery successfully identified ecosystems whereas an unsupervised method was not successful. Frazer (1998) found that a supervised classifier was better than an unsupervised one for mapping blackberry fields using high-resolution digital video data. Conversely, Thomson, *et al.* (1998) demonstrated that an ISODATA classifier performed better than a maximum likelihood classifier when

mapping coastal environments using Compact Airborne Spectrographic Imager (CASI) data. Bryant and Huber (1998) reported that an unsupervised classifier was marginally better than a supervised one for mapping pronghorn habitat, but that when PCA was used instead of raw data, the results were reversed. Lass and Callihan (1997) found that classifier method meant less to accuracy results than did the phenological stage of target vegetation in mapping weed infestations.

These mixed results suggest that there are benefits to both methods, and have led to development of hybrid approaches to classification that combine elements of supervised and unsupervised algorithms. Various hybrid methods have been tried since at least the early 1990s (Bauer, *et al.*, 1994), and refined in many cases (Cuevas-Jimenez, *et al.*, 2002; Reese, *et al.*, 2002; Turner and Congalton, 1998). Most hybrid methods involve 1) an initial stratification of the imagery by spectral clustering, 2) assignment of clusters to user-defined classes, and 3) maximum likelihood (or similar decision rule) classification of the entire image. Hybrid methods have proved to be valuable in analyses where there is complex variability in the spectral data within information classes, such as is commonly found in vegetation mapping (Lillesand and Kiefer, 2000).

The Iterative Guided Spectral Class Rejection (IGSCR) is a hybrid classifier whose proponents claim is fast, objective and repeatable across users (Wayman, *et al.*, 2001). The method uses specific rejection criteria and large numbers of training pixels to cluster similar pixels into two or three user-defined classes through a series of iterations (Musy, 2003; Wayman, *et al.*, 2001). The IGSCR method accepts and labels a spectral class when it meets a user defined inclusion threshold and rejects it if it does not. Rejected pixels are then classified in the next iteration and so on until a convergence threshold is met. Finally, these pure classes are used with a maximum-likelihood decision rule to classify the image into pre-defined information classes.

This paper presents two case studies evaluating these three classifiers: supervised/unsupervised and the IGSCR hybrid method proposed by Wayman, *et al.* (2001), for their accuracy in discriminating dead trees from the healthy forest mosaic surrounding them, while minimizing confusion with bare patches utilizing high resolution imagery. We also tested the sensitivity of the hybrid algorithm to changes in two important input parameters, homogeneity and ISODATA class number, and compared the benefits in accuracy between using pixel based training data or polygonal training data.

The paper concludes with a discussion of what we know about monitoring oak and tanoak mortality in areas affected by sudden oak death using high-resolution remotely sensed imagery, and provides a discussion concerning the advantages and remaining challenges faced by those monitoring the disease using remote sensing.

Study Areas

The two study areas discussed in this paper are considered to be "hot spots" for SOD (Svihra, 1999). The first, in Marin Municipal Water District (MMWD) (122°35′ W, 37°57′ N), is part of the hardwood and redwood/tanoak forest found in the interior of Marin County (Plate 1). MMWD has moderate to steep topography with elevations ranging from sea level at the Pacific Ocean to over 700 m. Other vegetation in the area includes mixed evergreen forest and chaparral communities on higher elevations. The area supports extensive wildlife, and is managed by the MMWD for moderate-use recreation and drinking water supply for nearby Marin County cities. Here, hosts for *P. ramorum* include tanoak (*Lithocarpus densiflorus*), redwood (*Sequoia sempervirens*), Douglas fir (*Pseudotsuga menziesii* v. *menziesii*), coast live oak (*Quercus agrifolia*), black oak (*Quercus kelloggii*), and numerous shrub species. It is important to note that tanoak and the two oak species are the only hosts that show the dramatic canopy color changed described earlier. The other species mentioned are defined as "foliar hosts" meaning that the pathogen attacks their leaves instead of causing the more extensive trunk cankers found on the *Quercus* and *Lithocarpus* individuals (Rizzo, *et al.*, 2002). These plants are suspected to be the most durable and persistent source of the pathogen, and during wind and rain events, the fungus can be dispersed from these foliar hosts to infect new trees (Davidson, *et al.*, 2002). These hosts are not commonly visible from above, and are not targets for monitoring via remote sensing. Targets for this study include the forest mosaic, bare areas, and dead tanoak and oaks crowns (Plate 2a).

China Camp State Park (CCSP), also in Marin County (122°29′ W, 38°00′ N), is a wooded peninsula on San Pablo Bay (Plate 1). The area has moderate to steep topography, with elevations ranging from sea level to over 300 m. The forest stands are near even-age stands as these hillsides were harvested for timber in the early to mid-1800s. Coast live (*Quercus agrifolia*), black (*Quercus kelloggii*), and valley oaks (*Quercus lobata*) are abundant, and occur in mixed stands with mature madrone (*Arbutus menziesii*) and California bay (*Umbellularia californica*) trees providing habitat to a variety of wildlife, including deer, squirrels, and numerous birds. All of these trees are hosts for *P. ramorum* with the exception of valley oak. It is the two *Quercus* species that were the targets for this study, along with bare areas and the forest mosaic (Plate 2b).

In each of these forests we located a rectangular shaped area and ground-truthed (using GPS and hardcopy imagery) all dead stems. In MMWD, the rectangle is 7.5 ha in size located approximately 450 m above sea level, and includes a mixed hardwood redwood stand. The CCSP study area covers approximately 5 ha and is located 20 m above sea level and is covered by hardwood forest.

Methods

Data and Imagery Evaluated

Digital imagery was acquired for the larger MMWD area and the larger CCSP area on 05 May 2001 with an ADAR5500 imaging system that was comprised of a 20 mm lens with four mounted cameras (Spectral Bands: Blue: 450–550 nm, Green: 520–610 nm, Red: 610–700 nm, Near Infrared (NIR): 780–920 nm) flown at an average aircraft altitude of 2,205 m. Imagery was acquired near Noon, in clear-sky conditions (solar elevation = 58.65°). We contracted with a private company (Positive Systems, Inc.) to perform the imagery acquisition and registration. RMSE was reported to be less than 1 m. The average ground spatial resolution of the images is 1 meter. Each 1,000 m × 1,500 m frame was captured with 35 percent end and 35 percent side-lap. Further information about the imagery can be found in Kelly (2002).

Pre-Processing

The individual image frames were color balanced, mosaiced, and then georeferenced to previously acquired and georeferenced ADAR images from Spring 2000. Those images had been georeferenced using a 16 cm resolution digital ortho-photograph of the entire county provided by Marin Municipal Water District. The contractor provided the image registration using in-house DIME© software. The georeferenced mosaics were clipped to the study area boundaries. All analysis was performed in Erdas Imagine® software (Erdas, 1999).

Classification

Three classifiers were evaluated for their accuracy in discriminating dead trees from the surrounding healthy forest mosaic while minimizing confusion with bare patches. First, a supervised classification of the study areas was performed on the

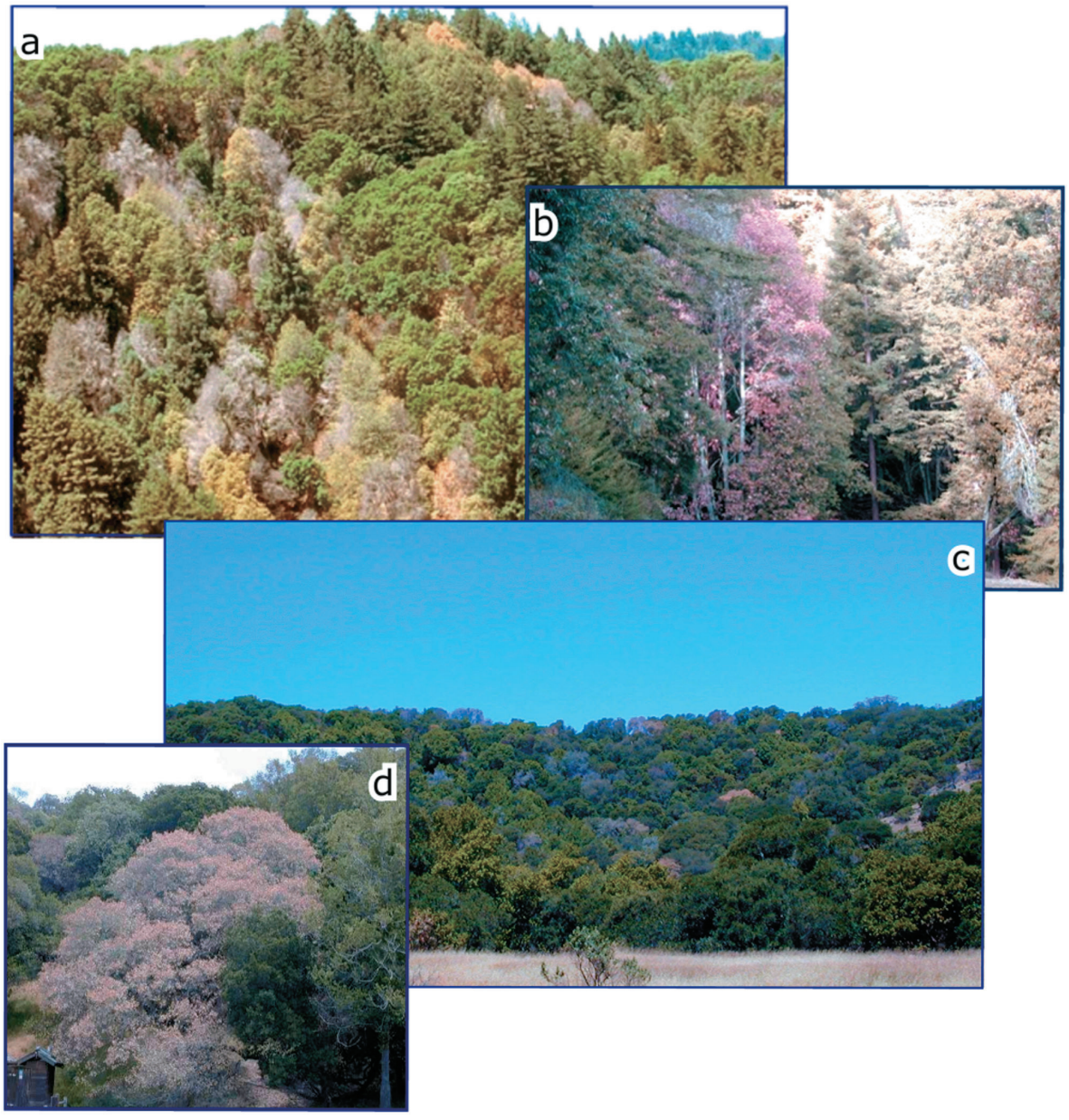

Plate 1. Examples of sudden oak death in California. Photograph (a) shows tanoak mortality in a mixed redwood—tanoak forest in Marin County. Photograph (b) shows the crown mortality and color change typically found on an affected tanoak tree. Photograph (c) shows Quercus mortality across a hillside, and photograph (d) shows the typical crown color change found on affected Quercus trees. For more examples, please see the website: http://www.suddenoakdeath.org; last date accessed 23 August 2004.

four ADAR bands (blue, green, red, and NIR) using training classes captured on screen. Training data for the supervised method were chosen for three information classes: dead crowns, bare areas, and forest mosaic in polygonal form using the Erdas Imagine® region growing routine constrained to the 4-neighbor case (Erdas, 1999). We found we had more control on the region growing procedure with the 4- rather than the 8-neighbor case. This tool collects the spectral properties of pixels spatially adjacent to seed pixels. A seed pixel is located on the image, and the Euclidean distance value is changed until the training area covered by the region covers the appropriate area on the image. Growth was terminated by the analyst before the region grown included pixels from a different information class. Once signatures were developed, a maximum likelihood classifier was used to cluster the image into 13 spectral classes in MMWD and 27 spectral classes in CCSP (these numbers corresponded to the overall number of training classes used in each image).

Second, an unsupervised classification of the areas was performed using the ISODATA routine over 25 iterations (the algorithm reached its convergence threshold in eight iterations in each study area) with eight classes as an output and a convergence threshold of 0.950. The ISODATA clustering routine uses the minimum distance formula to form spectrally distinct clusters (Erdas, 1999). The result was interpreted and the best combination of classes that corresponded to dead trees was then re-classed as dead and the remaining classes re-classed as forest or bare.

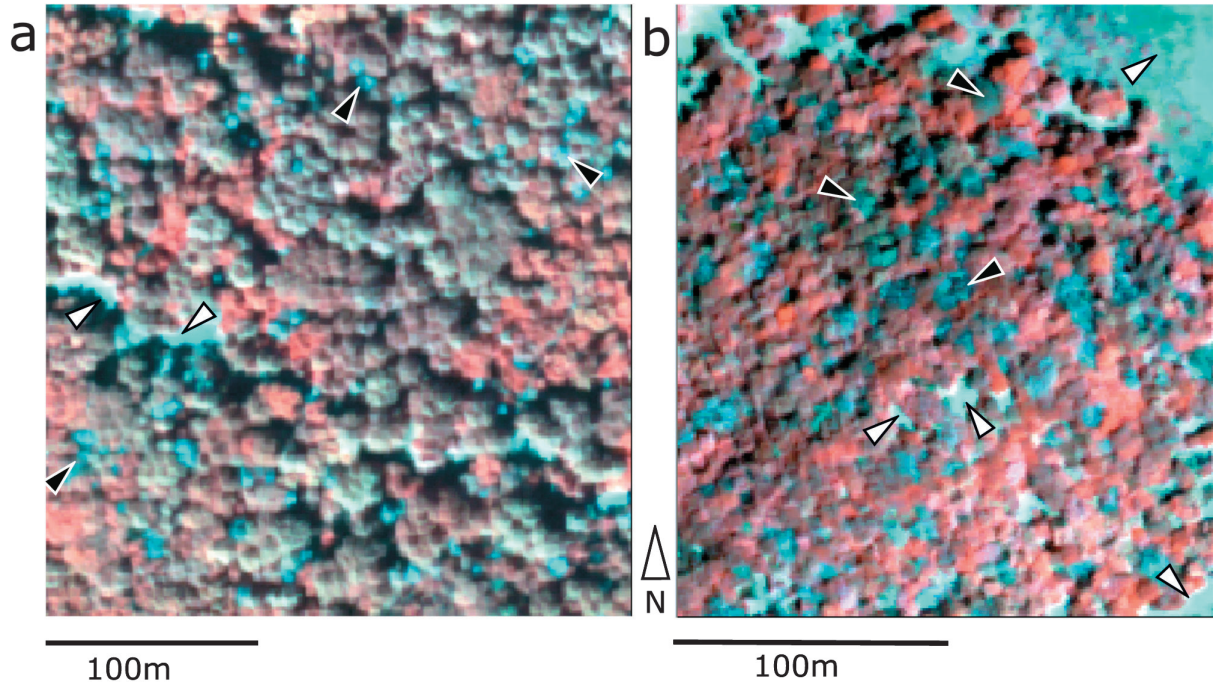

Plate 2. The study areas. Both graphics show ADAR imagery as a false color composite, with the NIR band shown in red. Image spatial resolution is 1 m. (a) MMWD: Trees at the center of the image are redwood and tanoak, grading to mixed hardwood to the middle right and southwest. Dead crowns are visible as gray to bluish circular features and are noted with black arrows. Bare areas are noted with white arrows. (b) CCSP: Note the bare area to the northeast corner and the small forest gaps noted by the white arrows. Dead crowns show as bluish gray on this image, and are noted by black arrows.

Finally, the IGSCR hybrid method was used to discriminate between the three classes based on mutually exclusive user-defined training data. Training data were gathered for forest, bare, and dead crowns using the region growing methods described above. We used an operational version of the IGSCR hybrid method algorithm written in Erdas Macro Language® (EML) and Erdas Imagine Toolkit® by Musy (2003). Parameters for the IGSCR algorithm include number of ISODATA classes, homogeneity threshold, and number of iterations. The IGSCR method first clustered the spectral data into a predetermined number of classes using the ISODATA algorithm. In the next iteration pixels were then extracted from the clustered image within training areas. A test of proportion was used on those pixel data to determine pixels that fall into a homogeneous class (a homogeneity threshold), and these "pure" pixels were masked out of the image. The remaining pixels were again clustered and "pure" pixels removed. This continued until either the homogeneity threshold or the iteration number was reached. Signatures gathered from the previous iterations were used with a maximum likelihood decision rule to classify the entire image (Musy, *et al.*, In review). For MMWD, we used a 90 percent homogeneity threshold with 3 ISODATA classes over 10 iterations. For CCSP, we used a 90 percent homogeneity threshold with 5 ISODATA classes over 10 iterations.

Accuracy Assessment Reference Data

In both study areas a set of dead crowns was manually digitized onto the image from the screen based on numerous field visits, and GPS data. Twice that number of points were randomly located throughout each image study area, but not in areas of dead crowns. We made sure that the number of the random points that fell on bare areas was in proportion to the total size of the bare areas. These points (dead, forest, and bare) were used to assess the accuracy of three classification methods. This yielded 165 points in MMWD (55 dead, 8 bare, and 102 forest), and 180 points (60 dead, 24 bare, and 96 forest) in CCSP. Aside from the dead crowns, which were determined as above, we chose randomly distributed points to avoid bias introduced by manual selection of the validation set (Debeir, *et al.*, 2002). These numbers of reference points are acceptable for expected accuracies greater than 85 percent and an allowable error of 5 percent given the formula for a binomial distribution presented in Jensen (1996).

Accuracy Assessment

Confusion matrices, kappa statistic, and Z-scores were used to assess the accuracy of each classifier (Congalton and Green, 1999; Foody, 2002; Hudson and Ramm, 1987). Prior to accuracy assessment, each classified product was recoded so that forest = 0, bare = 1, and dead = 2. A GridSpot© routine was used in ESRI ArcGIS® to determine the value of the pixel beneath each reference point. Overall accuracies, omission (Producer's), and commission errors (User's) were calculated for each study area for each classifier. A kappa statistic (or khat) and Z-score were also calculated for each individual classification, and a pairwise Z-score was calculated comparing each pair of classifiers according to the method outlined in Congalton and Green (1999). We provided all measures of accuracy to help alleviate some of the problems surrounding accuracy assessment detailed by Foody (2002).

Refining the Hybrid Method

We wanted to evaluate the hybrid classification method thoroughly, so we changed certain important input parameters in the program and tested responses. In their article introducing this algorithm, Wayman, *et al* (2001) recommend further research on the method, including (among others) the following specific points: 1) test effects of iteration number on

classification accuracy; 2) test the effect of homogeneity on the classification accuracy; 3) test effects of number of original ISODATA clusters in stage one of the algorithm on classification accuracy; and 4) explore maximizing the accuracy of the classification using a random subsample of training pixels, instead of a polygonal set of training data.

We tested the effect of the first three parameters (iteration number, number of ISODATA clusters, and homogeneity) directly by varying them sequentially and re-running the classification. We first varied the iteration number, trying 10, 20, and 100 iterations. Next we tested the effect of class number on classification results by varying the number of ISODATA classes in the first phase of the algorithm across three, five, 10, and 100 classes. We also varied the homogeneity threshold from 80 to 95 in increments of five. Once we found the optimum combination of parameters, we tested the influence of a random subsample of training points versus polygonal training samples derived from region growing on classification accuracy. We generated random points that represented approximately 1 percent of the size of the training area polygons delimited for forest mosaic, bare areas, and dead crowns. This represented 698 points for MMWD and 1,117 points for CCSP. While small in proportion, these absolute numbers of pixels constitute large numbers of individual training pixels when compared to studies such as Chen and Stow (2002), and meet the 10*n* pixel per class (where n = number of bands classified) requirement set in Jensen (1996). Total numbers of pixels for the study areas and for both training methods are available in Table 1. These pixels were used as the training areas in running the IGSCR algorithm using the parameters that yielded the most accurate results. Accuracy assessment was performed on these results as before.

TABLE 1. PIXEL NUMBERS FOR STUDY AREAS AND TRAINING METHODS

	MMWD	CCSP
Study area size (rows, columns)	270 × 280	200 × 229
Study area size (pixels)	76,140	45,800
Polygonal training data (pixels)		
Forest	6011	6892
Bare	154	3508
Dead	340	772
Total	6505	11172
Pixel training data		
Forest	601	689
Bare	42	351
Dead	55	77
Total	698	1117

TABLE 2. ACCURACY MATRICES FOR FOUR CLASSIFICATION METHODS—MMWD. BOLD NUMBERS INDICATE RESULTS ARE SIGNIFICANTLY BETTER THAN RANDOM CHANCE AT THE 95 PERCENT CONFIDENCE LEVEL

Supervised	Reference				
Classified	Forest	Bare	Dead		*User's*
Forest	100	0	0	100	1
Bare	1	8	18	27	0.296296
Dead	1	0	37	38	0.973684
	102	8	55	165	
Producer's	0.980392	1	0.672727	*Overall*	0.878788
				Khat	0.7758
				Z	**18.77986**
Unsupervised	Reference				
Classified	Forest	Bare	Dead		*User's*
Forest	85	0	5	90	0.944444
Bare	6	8	34	48	0.166667
Dead	11	0	16	27	0.592593
	102	8	55	165	
Producer's	0.833333	1	0.290909	*Overall*	0.660606
				Khat	0.428783
				Z	**9.061825**
IGSCR Hybrid	Reference				
Classified	Forest	Bare	Dead		*User's*
Forest	102	0	7	109	0.93578
Bare	0	7	0	7	1
Dead	0	1	48	49	0.979592
	102	8	55	165	
Producer's	1	0.875	0.872727	*Overall*	0.951515
				Khat	0.901168
				Z	**26.55938**

Results

Evaluation of Classifiers

In both study areas the hybrid classifier outperformed all other methods. However, there were differences between the study areas with respect to individual classifier performance. In MMWD, the unsupervised method provided the lowest overall accuracy (66.1 percent; kappa: 42.9 percent) with high errors of omission and commission (Table 2). This method produced considerable over-classification of dead pixels (Figure 2b). The supervised method increased accuracies (to 87.9 percent; kappa: 77.6 percent), but confusion remained between dead crowns and bare areas (Figure 2a). The hybrid method provided high accuracy (95.2 percent; kappa: 90.1 percent) with low omission and commission errors across classes (Figure 2c). This method provided the best visual interpretation of the original image; all bare patches (located in Plate 2a) are correctly distinguished from dead crowns. The hybrid method was significantly different (pairwise Z-scores of 2.4 and 8.1, respectively) from the supervised and unsupervised methods (Table 4).

In CCSP, the supervised classifier resulted in moderate accuracy (73.5 percent; kappa: 54.5 percent), with high errors of omission and commission, and confusion between the bare areas and dead crowns (Table 3). This classifier also provided considerable speckle to the final map (Figure 3a). The unsupervised classifier performed moderately well (78.8 percent; kappa: 66.6 percent), producing less speckle. It successfully mapped the open areas at the northeast corner of the study area, but there was still considerable confusion between dead and bare in the open areas at the southeast corner of the study area (Figure 3b). The hybrid method provided the best overall accuracy (93.2 percent; kappa: 88.4 percent) with low errors of omission and commission, and was significantly different from the supervised and unsupervised methods (pairwise Z-score of 5.4 and 4.1, respectively) (Table 4). The hybrid method successfully discriminated between the dead trees in the north of the study area with the similarly shaped bare areas toward the south (located in Plate 2b). There was still some confusion within the large bare area at the northeast corner of the study area with numerous pixels classified as dead (Figure 3c).

Refining the IGSCR Algorithm

We tested the sensitivity of the IGSCR method to changes in three important input parameters: number of iterations, homogeneity, and ISODATA class number. The effect of iteration

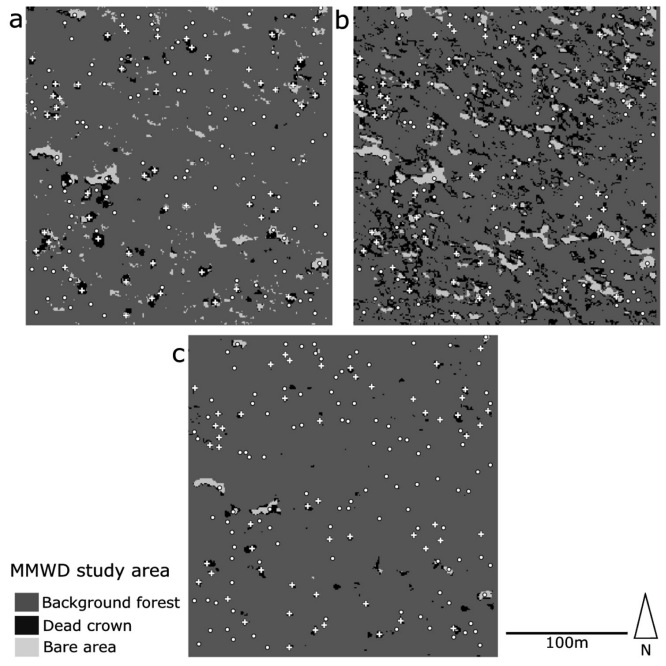

Figure 2. Classified images for the MMWD study area. (a) Supervised classifier, (b) unsupervised classifier and (c) hybrid IGSCR method.

TABLE 3. ACCURACY MATRICES FOR FOUR CLASSIFICATION METHODS—CCSP. BOLD NUMBERS INDICATE RESULTS ARE SIGNIFICANTLY BETTER THAN RANDOM CHANCE AT THE 95 PERCENT CONFIDENCE LEVEL

Supervised	Reference				
Classified	Forest	Bare	Dead		*User's*
Forest	82	0	30	112	0.732143
Bare	13	22	2	37	0.594595
Dead	2	1	29	32	0.90625
	97	23	61	181	
Producer's	0.845361	0.956522	0.47541	*Overall*	0.734807
				Khat	0.544988
				Z	**9.90997**

Unsupervised	Reference				
Classified	Forest	Bare	Dead		*User's*
Forest	88	0	4	92	0.956522
Bare	9	7	0	16	0.4375
Dead	0	16	57	73	0.780822
	97	23	61	181	
Producer's	0.907216	0.304348	0.934426	*Overall*	0.788889
				Khat	0.666488
				Z	**15.74424**

IGSCR Hybrid	Reference				
Classified	Forest	Bare	Dead		*User's*
Forest	92	2	1	95	0.968421
Bare	3	20	3	26	0.769231
Dead	2	1	53	56	0.946429
	97	23	57	177	
Producer's	0.948454	0.869565	0.929825	*Overall*	0.932203
				Khat	0.884086
				Z	**27.74997**

TABLE 4. PAIRWISE COMPARISON OF ERROR MATRICES FOR ALL CLASSIFIERS. BOLD RESULTS ARE SIGNIFICANT AT THE 95 PERCENT CONFIDENCE LEVEL

Pairwise Comparison—MMWD			
	SUP	UNSUP	Hybrid
SUP	0		
UNSUP	**5.525**	0	
Hybrid	**2.345**	**8.113**	0

Pairwise Comparison—CCSP			
	SUP	UNSUP	Hybrid
SUP	0		
UNSUP	1.751	0	
Hybrid	**5.335**	**4.107**	0

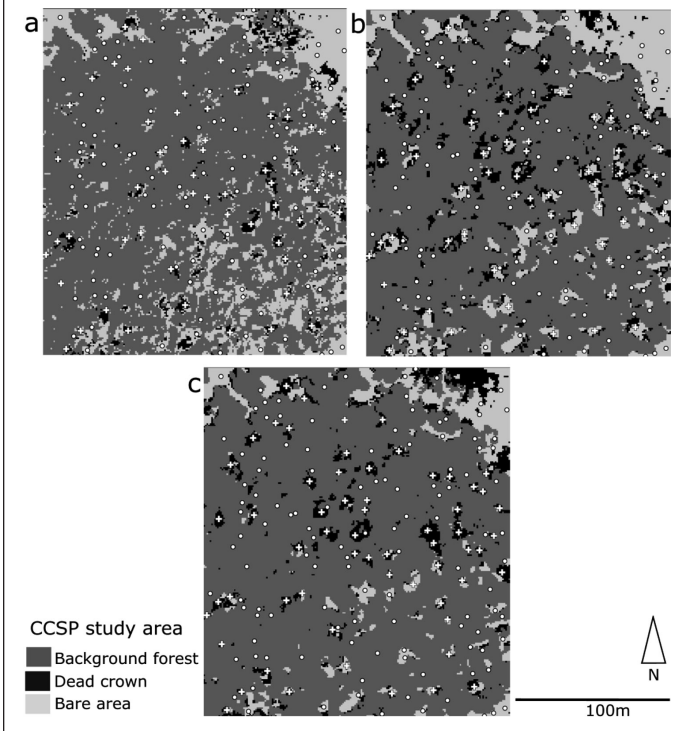

Figure 3. Classified images for the CCSP study area. (a) supervised classifier, (b) unsupervised classifier and (c) hybrid IGSCR method.

number was tested first, and it was found that iteration numbers greater than 10 produced identical results to those with 10 iterations. We then tested the effect of class number on classification results by varying the number of ISODATA classes in the first phase of the algorithm across three, five, 10, and 100 classes. We also varied the homogeneity threshold from 80 to 95 in increments of five. This produced 16 runs of the IGSCR model for each study area.

For MMWD, the three-class option with 90 percent homogeneity threshold provided the best overall accuracy results (95.2 percent) (Figure 4a), and best kappa statistic (90.8 percent) (Figure 5a), although it was not possible to test the algorithm with three classes at the 80 percent homogeneity threshold. IGSCR with 10 classes provided the poorest overall accuracies and kappa statistics from 80 to 90 percent homogeneity threshold; the five-class option peaked in accuracy

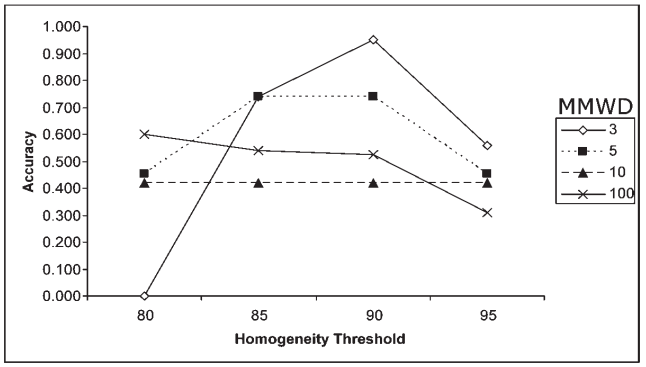

(a)

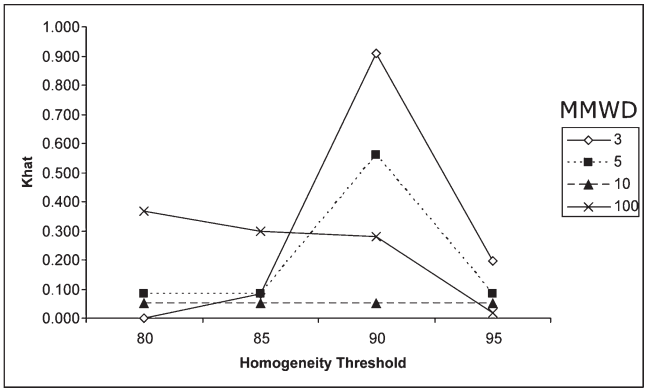

(b)

Figure 4. (a) Overall accuracy vs. homogeneity threshold for 3, 5, 10 and 100 classes—MMWD, (b) kappa statistic vs. homogeneity threshold for 3, 5, 10 and 100 classes—MMWD.

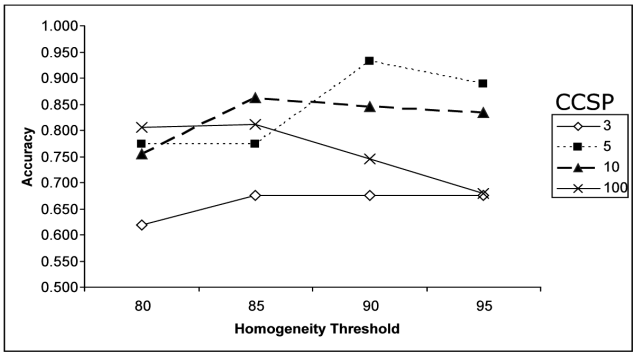

(a)

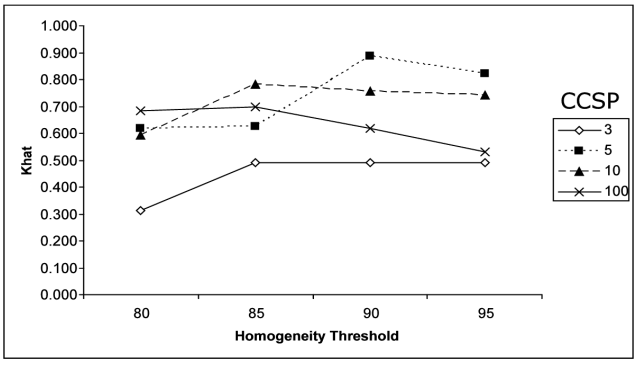

(b)

Figure 5. (a) Overall accuracy vs. homogeneity threshold for 3, 5, 10 and 100 classes—CCSP, (b) kappa statistic versus homogeneity threshold for 3, 5, 10 and 100 classes—CCSP.

with 85 percent homogeneity threshold, and then declined. The 100-class option provided poor accuracies with the homogeneity threshold at 80 percent, and declined from there. These results were reflected in the pairwise testing of significance: the three-class, 90 percent-homogeneity threshold run was significantly better than all others (Table 5), and the three-class, 95 percent-homogeneity threshold run was better than all others except the three class, 90 percent-homogeneity threshold run.

For CCSP, the five-class option produced the best overall results (93.2 percent) and kappa statistic (88.8 percent) with a homogeneity threshold of 90 percent (Figure 4). IGSCR with three classes provided the worst accuracies across all homogeneity thresholds. Ten classes provided moderate accuracies above the 85 percent homogeneity threshold, while the accuracy of the algorithm with 100 classes peaked at 80 percent homogeneity threshold and declined thereafter. Again, these results are reflected in the pairwise testing of significance (Table 5). The five-class, 90 percent-homogeneity threshold run was significantly better than all others, the three-class, 95 percent-homogeneity threshold run was better than all others at the 95 percent homogeneity threshold, and runs with three classes were significantly worse than all others.

IGSCR classification using random training pixels provided significantly lower accuracy than classification using polygonal training sites in both study areas. MMWD classification using random training pixels yielded 21.2 percent overall accuracy, and in CCSP yielded 44.7 percent overall accuracy (Table 6). These results were significantly different at the 95 percent confidence level from the classification with polynomial training data (pairwise Z-score for MMWD = 11.77, for CCSP = 9.15) using the formula for pairwise comparison of error matrices provided by Congalton and Green (1999).

Discussion

Supervised and unsupervised classification of raw band imagery did not yield high accuracy rates, even when the goal of classification was not complex species mapping, but rather a simplistic discrimination between dead crowns, forest mosaic, and bare areas. Utilizing both methods produced considerable confusion between dead crowns and bare areas in the two study areas. None of the classifiers evaluated, other than the hybrid method, performed consistently across study areas. In the redwood-tanoak-hardwood forest of MMWD, the supervised classifier performed better than the unsupervised method; the reverse was true in the hardwood forest of CCSP. The hybrid method outperformed the other methods significantly. In MMWD, the hybrid method successfully pulled apart the bare patches on the left side of the image from the bare crowns throughout the northeast corner. All other methods confused the two features. For CCSP, the hybrid method performed better than the other methods, and discriminated between bare areas and dead crowns in the interior of the forest, while maintaining some confusion in the extensive bare areas to the northeast of the study area. We do not feel that this is an insurmountable problem, as we can remove large areas of pixels classified as dead surrounded by bare areas with a simple search by size.

We tested parameter influence on accuracy suggested by Wayman, *et al.* (2001). They recommend testing the effects of iteration number, homogeneity threshold, the number of original ISODATA clusters in stage one of the algorithm, and

TABLE 5. PAIRWISE COMPARISON OF ERROR MATRICES FOR HYBRID CLASSIFIERS. BOLD RESULTS ARE SIGNIFICANT AT THE 95 PERCENT CONFIDENCE LEVEL

Pairwise Comparison (class, homogeneity threshold)—MMWD

	3,80	3,85	3,90	3,95	5,80	5,85	5,90	5,95	10,80	10,85	10,90	10,95	100,80	100,85	100,90	100,95
3,80	0.00															
3,85	n.a.	0.00														
3,90	n.a.	**13.51**	0.00													
3,95	n.a.	**2.12**	**12.14**	0.00												
5,80	n.a.	0.00	**13.51**	**2.12**	0.00											
5,85	n.a.	0.00	**13.51**	**2.12**	0.00	0.00										
5,90	n.a.	**5.08**	**5.58**	**3.50**	**5.08**	**5.08**	0.00									
5,95	n.a.	0.00	**13.51**	**2.12**	0.00	0.00	**5.08**	0.00								
10,80	n.a.	0.54	**13.55**	**2.61**	0.54	0.54	**5.42**	0.54	0.00							
10,85	n.a.	0.54	**13.55**	**2.61**	0.54	0.54	**5.42**	0.54	0.00	0.00						
10,90	n.a.	0.54	**13.55**	**2.61**	0.54	0.54	**5.42**	0.54	0.00	0.00	0.00					
10,95	n.a.	0.54	**13.55**	**2.61**	0.54	0.54	**5.42**	0.54	0.00	0.00	0.00	0.00				
100,80	n.a.	**2.59**	**7.70**	0.99	**2.59**	**2.59**	**2.02**	**2.59**	**2.99**	**2.99**	**2.99**	**2.99**	0.00			
100,85	n.a.	1.65	**8.33**	0.06	1.65	1.65	**2.74**	1.65	**2.05**	**2.05**	**2.05**	**2.05**	0.76	0.00		
100,90	n.a.	1.32	**8.15**	0.21	1.32	1.32	**2.87**	1.32	1.71	1.71	1.71	1.71	0.95	0.22	0.00	
100,95	n.a.	1.26	**10.12**	**2.74**	1.26	1.26	**4.99**	1.26	0.85	0.85	0.85	0.85	**3.13**	**2.39**	**2.12**	0.00

Pairwise Comparison (class, homogeneity threshold)—CCSP

	3,80	3,85	3,90	3,95	5,80	5,85	5,90	5,95	10,80	10,85	10,90	10,95	100,80	100,85	100,90	100,95
3,80	0.00															
3,85	1.32	0.00														
3,90	1.32	0.00	0.00													
3,95	1.32	0.00	0.00	0.00												
5,80	**4.53**	**2.46**	**2.46**	**2.46**	0.00											
5,85	**4.62**	**2.52**	**2.52**	**2.52**	0.07	0.00										
5,90	**10.08**	**6.54**	**6.54**	**6.54**	**4.70**	**4.63**	0.00									
5,95	**8.03**	**5.19**	**5.19**	**5.19**	**3.14**	**3.07**	1.40	0.00								
10,80	**3.95**	**2.04**	**2.04**	**2.04**	0.43	0.50	**5.01**	**3.49**	0.00							
10,85	**6.99**	**4.45**	**4.45**	**4.45**	**2.31**	**2.24**	**2.16**	0.76	**2.68**	0.00						
10,90	**6.40**	**4.02**	**4.02**	**4.02**	1.84	1.77	**2.59**	1.19	**2.21**	0.43	0.00					
10,95	**6.05**	**3.75**	**3.75**	**3.75**	1.54	1.47	**2.88**	1.48	1.92	0.72	0.28	0.00				
100,80	**4.73**	**2.84**	**2.84**	**2.84**	0.63	0.57	**3.45**	**2.16**	1.01	1.45	1.04	0.77	0.00			
100,85	**5.02**	**3.04**	**3.04**	**3.04**	0.84	0.77	**3.32**	**2.00**	1.21	1.28	0.86	0.60	0.18	0.00		
100,90	**3.49**	1.73	1.73	1.73	0.69	0.76	**5.06**	**3.62**	0.27	**2.84**	**2.40**	**2.12**	1.23	1.43	0.00	
100,95	1.88	0.38	0.38	0.38	**2.22**	**2.30**	**6.72**	**5.20**	1.77	**4.38**	**3.91**	**3.62**	**2.64**	**2.86**	1.45	0.00

TABLE 6. ACCURACY MATRICES FOR POLYGONAL VERSUS PIXEL-BASED TRAINING CLASSIFIERS

MMWD	Reference				
Classified	Forest	Bare	Dead		*User's*
Forest	35	0	7	42	0.833333
Bare	0	0	48	48	0
Dead	67	8	0	75	0
	102	8	55	165	
Producer's	0.343137	0	0	*Overall*	0.212121
				Khat	−0.16374
				Z	−4.73765

CCSP	Reference				
Classified	Forest	Bare	Dead		*User's*
Forest	32	0	0	32	1
Bare	3	21	33	57	0.368421
Dead	62	2	28	92	0.304348
	97	23	61	181	
Producer's	0.329897	0.9130435	0.459016	*Overall*	0.447514
				Khat	0.203836
				Z	**4.206182**

use of a random subsample of training pixels on classification accuracy. By varying the hybrid algorithm parameters we were able to determine the best combination for classification accuracy for each study area. The best combination of parameters varied by study area; MMWD required a three class, 90 percent homogeneity threshold, and CCSP a five class, 90 percent homogeneity threshold. These results imply that before final classification with the hybrid method one should find the optimum combination of input parameters. We then used these class and homogeneity threshold combinations to determine the effect of randomly located training points versus polygonal training samples derived from region growing. Classification using random training points did not yield high accuracies. Our results contradict several recent studies examining pixel versus polygon training areas, most notably Chen and Stow (2002) who found the seed method used here to be the worst performer. We cannot completely explain the difference in results here. The different land cover of the studies might play a role (i.e., Chen and Stow concentrated in urban environments), but probably more important is our conjecture that since the IGSCR method requires large numbers of training pixels, and randomly choosing pixels from training polygons by definition reduces the number of training pixels used in the classifier, the number of pixels plays a role in accuracy. Indeed, this has been observed by Chen and Stow (2002), who suggest that only with the most homogeneous classes can a small number of training pixels be used. The random points used here cover approximately 1 percent of the area found in the polygonal training areas, but, while small in proportion, we note that the absolute numbers of pixels used in the pixel based training method was far greater than those used by

Chen and Stow (2002), and approximated the 10*n* pixels per class general rule (*n* being the number of bands being classified) presented in Jensen (1996) and elsewhere.

In this paper we also answer two of the additional questions posed by Wayman, *et al*. (2001). They suggested a comparison between use of the maximum-likelihood classifier on the IGSCR results and use of maximum-likelihood on the unclassified pixels alone. We show that in our study areas, maximum likelihood with IGSCR out-performs maximum likelihood used on raw data. They also suggest trying the IGSCR approach in different physiographic regions of the United States and in areas of rapid change. We have shown that the approach works well in a different area, and with a different sensor. We plan to use the method to examine the change in the area caused by the disease.

Conclusions

High-resolution 4-band imagery (1 meter spatial resolution) proved to be useful for mapping tree mortality in areas affected by the pathogen *P. ramorum*. Because the late stage of the disease results in such a dramatic spectral reflectance shift across the visible to NIR range, classification of spectral data can be used as a method to distinguish dead crowns from other features. However, the method is not straightforward, and standard spectral classification methods (such as, ISODATA or maximum likelihood) on raw data alone do not provide high classification accuracies. In both study areas examined, a hybrid classifier outperformed all other methods. The ability of standard supervised and unsupervised spectral classifications using only raw imagery to produce highly accurate maps of crown mortality is limited. The hybrid method, which combines features of both supervised and unsupervised classifiers performed much better, yielding accuracy that could be used in an operational monitoring program. Other more complex methods of classification (e.g., neural networks, contextual methods (Berberoglu, *et al*., 2000), and fuzzy classifications (Townsend and Walsh, 2001)) are being evaluated.

Acknowledgments

This work was supported by a NASA New Investigator award, and by a grant from the California Department of Forestry and Fire Protection, both to M. Kelly. The authors would like to thank R. Wynne and J. B. Campbell information about the IGSCR algorithm, and R. Musy for the Erdas® toolkit customization assistance. Contact Dr. Randolph Wynne (wynne@vt.edu) for more information on the module. Faith Kearns provided valuable editing and three anonymous reviewers helped strengthen the paper.

References

Barr, S., and M. Barnsley, 2000. Reducing structural clutter in land cover classifications of high spatial resolution remotely-sensed images for urban land use mapping, *Computers & Geosciences*, 26(4):433–449.

Bauer, M.E., T.E. Burk, A.R. Ek, P.R. Coppin, S.D. Lime, T.A. Walsh, D.K. Walters, W. Belfort, and D.F. Heinzen, 1994. Satellite inventory of Minnesota forest resources, *Photogrammetric Engineering & Remote Sensing*, 60(3):287–298.

Berberoglu, S., C.D. Lloyd, P.M. Atkinson, and P.J. Curran, 2000. The integration of spectral and textural information using neural networks for land cover mapping in the Mediterranean, *Computers & Geosciences*, 26(4):385–396.

Boyer, M., J. Miller, M. Belanger, and E. Hare, 1988. Senescence and spectral reflectance in leaves of northern pin oak (*Quercus palustris Muenchh*.), *Remote Sensing of Environment*, 25:71–87.

Bryant, F.C., and G.E. Huber, 1998. Classification of pronghorn fawning habitat using Landsat Thematic Mapper data, *Texas Journal of Science*, 50(1):3–16.

Campbell, J.B., 1981. Spatial correlation effects upon accuracy of supervised classification of land cover, *Photogrammetric Engineering & Remote Sensing*, 47(3):355–363.

Chen, D., and D. Stow, 2002. The effect of training strategies on supervised classification at different spatial resolutions, *Photogrammetric Engineering & Remote Sensing*, 68(11):1155–1162.

Congalton, R.C., and K. Green, 1999. *Assessing the Accuracy of Remotely Sensed Data: Principles and Practices*, CRC Press, Inc., Boca Raton, Florida, 137 pp.

Cuevas-Jimenez, A., P.-L. Ardisson, and A.R. Condal, 2002. Mapping of shallow coral reefs by colour aerial photography, *International Journal of Remote Sensing*, 23(18):3697–3712.

Davidson, J.M., D.M. Rizzo, M. Garbelotto, S. Tjosvold, and G.W. Slaughter, 2002. *Phytophthora ramorum* and sudden oak death in California: II. Transmission and survival, Fifth Symposium on Oak Woodlands, USDA-Forest Service, San Diego, California.

Debeir, O., I. VandenSteen, P. Latinne, P.V. Ham, and E. Wolff, 2002. Textural and contextural land-cover classification using single and multiple classifier systems, *Photogrammetric Engineering & Remote Sensing*, 68(6):597–606.

Egbert, S.L., S. Park, K.P. Price, R.-Y. Lee, J. Wuc, and M.D. Nellis, 2002. Using conservation reserve program maps derived from satellite imagery to characterize landscape structure, *Computers and Electronics in Agriculture*, 37(1-3):141–156.

Erdas, 1999. *Erdas Field Guide*, Erdas Inc., Atlanta, Georgia, 672 pp.

Everitt, J., D. Escobar, D. Appel, W. Riggs, and M. Davis, 1999. Using airborne digital imagery for detecting oak wilt disease, *Plant Disease*, 83(6):502–505.

Foody, G.M., 2002. Status of land cover classification accuracy assessment, *Remote Sensing of Environment*, 80(1):185–201.

Frazer, P., 1998. Mapping blackberry thickets in the Kosciuszko National Park using airborne video data, *Plant Protection Quarterly*, 13(3):145–148.

Gong, P., and P.J. Howarth, 1990. An assessment of some factors influencing multispectral land cover classification, *Photogrammetric Engineering & Remote Sensing*, 56(5):597–603.

Gong, P., X. Mei, G.S. Biging, and Z. Zhang, 1999. Monitoring oak woodland change using digital photogrammetry, *Journal of Remote Sensing*, 3(4):285–289.

Hudson, W.D., and C.W. Ramm, 1987. Correct formulation of Kappa coefficient of agreement, *Photogrammetric Engineering & Remote Sensing*, 53:421–422.

Jensen, J.R., 1996. *Introductory Digital Image Processing: A Remote Sensing Perspective*, Second Edition, Prentice Hall, Upper Saddle River, New Jersey, 318 pp.

Kelly, M., and R.K. Meentemeyer, 2002. Landscape dynamics of the spread of Sudden Oak Death, *Photogrammetric Engineering & Remote Sensing*, 68(10):1001–1009.

Kelly, N.M., 2002. Monitoring Sudden Oak Death in California using high-resolution imagery, USDA-Forest Service General Technical Report PSW-GTR-184, pp. 799–810.

Kelly, N.M., and B.A. McPherson, 2001. Multi-scale approaches taken to Sudden Oak Death monitoring, *California Agriculture*, 55(1): 15–16.

Lass, L.W., and R.H. Callihan, 1997. The effect of phenological stage on detectability of yellow hawkweed (*Hieracium pratense*) and oxeye daisy (*Crysanthemum leucanthemum*) with remote multispectral digital imagery, *Weed Technology*, 11(2):248–256.

Lillesand, T.M., and R.W. Kiefer, 2000. *Remote Sensing and Image Interpretation*, John Wiley and Sons, New York, 724 pp.

Lucas, R.M., M. Honzak, P.J. Curran, G.M. Foody, R. Milne, T. Brown, and S. Amaral, 2000. Mapping the regional extent of tropical forest regeneration stages in the Brazilian Legal Amazon using NOAA AVHRR data, *International Journal of Remote Sensing*, 21(15):2855–2881.

Lunetta, R.S., R. Alvarez, C.M. Edmonds, J.G. Lyon, C.D. Elvidge, R. Bonifaz, and C. Garcia, 2002. NALC/Mexico land-cover mapping results: Implications for assessing landscape condition, *International Journal of Remote Sensing*, 23(16):3129–3148.

Martinez-Casasnovas, J.A., 2000. A cartographic and database approach for land cover/use mapping and generalization from

remotely sensed data, *International Journal of Remote Sensing*, 21(9):1825–1842.

Miller, J.D., and S.R. Yool, 2002. Mapping forest post-fire canopy consumption in several overstory types using multi-temporal Landsat TM and ETM data, *Remote Sensing of Environment*, 82(2-3):481–496.

Muchoney, D.M., and B.N. Haack, 1994. Change detection for monitoring forest defoliation, *Photogrammetric Engineering & Remote Sensing*, 60(10):1243–1251.

Muchoney, D.M., and A.H. Strahler, 2002. Pixel- and site-based calibration and validation methods for evaluating supervised classification of remotely sensed data, *Remote Sensing of Environment*, 81(2-3):290–299.

Musy, R.F., 2003. Refinement of automated forest area estimation via iterative guided spectral class rejection. Master of Science Thesis, Virginia Polytechnic Institute and State University, Blacksburg, Virginia, 128 pp.

Musy, R.F., R.H. Wynne, C.E. Blinn, and J.A. Scrivani, In review. Automation of iterative guided spectral class rejection with the incorporation of a proportionality test on spectral class homogeneity, *Computers and Geosciences*.

Nagendra, H., and M. Gadgil, 1999. Satellite imagery as a tool for monitoring species diversity: An assessment, *Journal of Applied Ecology*, 36(3):388–397.

Reese, H., M. Nilsson, P. Sandström, and H. Olsson, 2002. Applications using estimates of forest parameters derived from satellite and forest inventory data, *Computers and Electronics in Agriculture*, 37(1-3):37–55.

Rizzo, D., M. Garbelotto, J.M. Davidson, G.W. Slaughter, and S.T. Koike, 2002. *Phytophthora ramorum* as the cause of extensive mortality of *Quercus* spp. and Lithocarpus densiflorus in California, *Plant Disease*, 86(3):205–213.

Rizzo, D.M., and M. Garbelotto, 2003. Sudden oak death: Endangering California and Oregon forest ecosystems, *Frontiers in Ecology and the Environment*, 1(5):197–204.

Svihra, P., 1999. Tanoak and coast live oak under attack, *Oaks 'n' folks*, 14(2):1.

Thomson, A.G., R.M. Fuller, and J.A. Eastwood, 1998. Supervised versus unsupervised methods for classification of coasts and river corridors from airborne remote sensing, *International Journal of Remote Sensing*, 19(17):3423–3431.

Townsend, P.A., and S.J. Walsh, 2001. Remote sensing of forested wetlands: Application of multitemporal and multispectral satellite imagery to determine plant community composition and structure in southeastern USA, *Plant Ecology*, 157:129–149.

Turner, M.D., and R.G. Congalton, 1998. Classification of multitemporal SPOT-XS satellite data for mapping rice fields on a West African floodplain, *International Journal of Remote Sensing*, 19(1):21–41.

Wang, S., J. Xu, and C. Zhou, 2002. Using remote sensing to estimate the change of carbon storage: A case study in the estuary of Yellow River delta, *International Journal of Remote Sensing*, 23(8):1565–1580.

Wayman, J., R. Wynne, J. Scrivani, and G. Reams, 2001. Landsat TM-based forest area estimation using iterative guided spectral class rejection, *Photogrammetric Engineering & Remote Sensing*, 67(10):1155–1166.

Xiao, X., S. Boles, J. Liu, D. Zhuang, and M. Liu, 2002. Characterization of forest types in Northeastern China, using multi-temporal SPOT-4 VEGETATION sensor data, *International Journal of Remote Sensing*, 23(18):3579–3594.

(Received 04 June 2003; accepted 29 August 2003; revised 25 September 2003)